National University of Science and Technology "POLITEHNICA" Bucharest
University Center of Pitesti
Faculty of Mechanics and Technology

SCIENTIFIC BULLETIN
AUTOMOTIVE series
year XXX, no. 34

Development of a tool to analyse adhesive volumes under X-ray µ-tomography

Andreea TINTATU[1*], Claudiu BADULESCU[2]

[1] Faculty of Mechanics and Technology, National University of Science and Technology Politehnica Bucharest, Bucharest, 060042, Romania
[2]Dupuy de Lôme Research Institute (IRDL), UMR CNRS 6027, ENSTA, Brest, F-29200, France

*Corresponding author e-mail andreea.tintatu@upb.ro

Article history
Received 15.07.2024
Accepted 12.10.2024

DOI https://doi.org/10.26825/bup.ar.2024.004

Abstract. In bonded assemblies, porosity within the adhesive layer— which often occurs during resin and hardener mixing—can significantly influence mechanical performance. This study addresses the lack of understanding regarding the effect of porosity on joint behavior by proposing a dedicated analysis methodology. A tool was developed to process X-ray µ-tomography data, allowing for noise filtering, artifact removal, and detection of microstructural entities (pores) through grayscale intensity thresholding. Two methods for average intensity extraction were designed and tested on synthetic volumes using MATLAB, with the more computationally efficient approach selected for real data analysis. This tool enables optimized porosity quantification, contributing to improved evaluation of adhesive joint integrity.
Keywords: bonded joint, structural assemblies, pores, analysis tool, X-ray µ-tomography

INTRODUCTION

In the design and fabrication of modern structures, the assembly of components represents a critical step with respect to the durability and reliability of the final structure. Classical mechanical joining techniques, such as bolting, riveting, or welding, have long been widely used across various industries. However, these methods can become inadequate or even unfeasible when dealing with complex geometries or dissimilar materials that are sensitive to temperature or localized stress concentrations. In this context, structural adhesive bonding has gained increasing prominence, offering an efficient and viable alternative to traditional joining techniques.

Adhesive bonding technology enables the creation of effective joints between different types of materials (composites, metal alloys, polymers, etc.) and is widely used in automotive, aerospace, marine, and railway industries. Among its notable advantages are a more uniform stress distribution, reduced stress concentrations, preservation of part geometry, and the ability to incorporate additional functionalities such as sealing or thermal/acoustic insulation [1]. However, despite these evident benefits, the mechanical behavior of bonded joints remains only partially understood, particularly in the presence of internal defects such as porosities [2-4].

Porosities are among the most common defects encountered in two-component adhesives. They often appear during the mixing process of resin and hardener and can increase in volume and size during the curing phase. These pores can significantly influence the mechanical behavior of the joint. Recent studies [5-6] have shown that such defects can serve as crack initiation sites, compromising both static and dynamic load-bearing capacity. Therefore, understanding how porosities affect the performance of bonded joints is essential for enhancing their reliability.

In this regard, the non-destructive analysis of the adhesive's microstructure, particularly via X-ray computed tomography (XCT), has become an especially valuable method [7]. Unlike conventional optical or electron microscopy—which provide only 2D images and require destructive

sample preparation—X-ray tomography enables the acquisition of high-resolution three-dimensional images of internal structures without compromising specimen integrity. This allows not only for the visualization of porosities but also for their quantification in terms of number, size, spatial distribution, and volume fraction [6]. Additionally, advances in 3D image processing software (such as ImageJ, VGStudio MAX, or Avizo) now facilitate semi- or fully-automated analysis of reconstructed volumes. These digital tools enable the extraction of quantitative data necessary for correlating defect presence with the mechanical behavior observed during experimental testing.

The main motivation for this study stems from the need to deeply analyze the influence of porosity on structural adhesive joints, with the main of developing a digital tool capable of processing volumes obtained through X-ray tomography and extracting and interpreting relevant microstructural parameters.

Accordingly, this work proposes the development and implementation of a tomographic data processing algorithm, which will include filtering steps, artifact correction and pore segmentation based on an intensity threshold. In addition, a robust method to determine the mean image intensity, which is essential for accurate pore boundaries, will be pursued. The proposed methodology will be tested on synthetic (simulated) volumes thus allowing the validation and practical application of the developed tool on real (experimentally obtained) volumes.

MATERIAL AND EXPERIMENTAL METHODS

The experimental method for investigating the porosity evolution in bonded assemblies using X-ray microtomography has been more extensively discussed in papers [8]. To achieve this, samples were prepared from two aluminum substrates bonded with a 400 µm layer of epoxy adhesive. The bonding process was carefully controlled using a custom device to ensure proper alignment and consistent adhesive thickness. Surface treatments were applied to improve adhesion, and the samples were cured in a thermal chamber at 115°C.

X-ray microtomography was then used to scan the samples while applying mechanical stress through a built-in tensile test machine. The scanning setup produced high-resolution 3D images that captured internal structural changes under load. The mechanical load was gradually increased in steps of 170 N until the samples failed.

Due to the large size of the reconstructed volumes, the complete study of microstructure in relation to the applied load requires the development of a processing tool that:

- Eliminates unwanted artifacts from reconstructed adhesive slices and extracts the average intensity;
- Filters the signal to eliminate noise;
- Detects observed microstructural features (porosities) from a grayscale intensity threshold.

The development of this analysis tool is the subject of the present article, and the methods of implementation are presented below.

CREATION OF A SYNTHETIC MICRO-TOMOGRAPHIC VOLUME

X-rays are generated during the acquisition at the microtomographic analysis. From this set of X-rays to which references and zero flux images are associated, we obtain projections of the attenuation constant μ considered as a continuous function of three spatial variables (x, y, z), which can be computed as follows:

$$\frac{I}{I_0} = \exp\left(\int \mu(x,y,z)dx\right) \quad (1)$$

Where:

- I_0 represents the intensity of the source;
- I is the detected intensity;
- $\boldsymbol{x}$ represents the distance along the transmission path.

To process tomographic images accurately, we express the gray levels S of each pixel in a volume slice in the following form:

$$S_{Z_j}(x,y) = I_{0,Z_j}(x,y) + \gamma_i . p_i(x,y) + b_{Z_j}(x,y) \quad (2)$$

In equation (2), the following quantities are used:

- $S_{Z_j}(x,y)$ represents the gray level, where j is the number of the slice in the Z direction of the studied volume, $j \in [0,1,\ldots,100]$;
- $I_{0,Z_j}(x,y)$ is the average intensity;
- γ_i represents the contrast for each phase;
- $p_i(x,y) = N_i$, où $N_i \in [0,1,\ldots,2^8-1]$ are integer values representing the gray level intensity of each phase, and $i \in [0,1,\ldots,N]$, where N is an integer representing the number of phases;
- $b_{Z_j}(x,y)$ is the random noise.

It is possible to establish the main architecture of this tool which consists of preprocessing images, extracting I_0 and analyzing these images, from the definition of its objective and the expression of the gray levels in relation to the coordinates of the pixels. In this context, the tool will be developed based on raw microtomographic images, such as shown in Figure 1a. Using this initial data, the tool will enable the automatic detection of relevant microstructural features in the raw signal, as exemplified in Figure 1b - the signal representing the gray levels along a path in the source image. After extracting the average intensity I_0 the identification of porosities and adhesive will be possible.

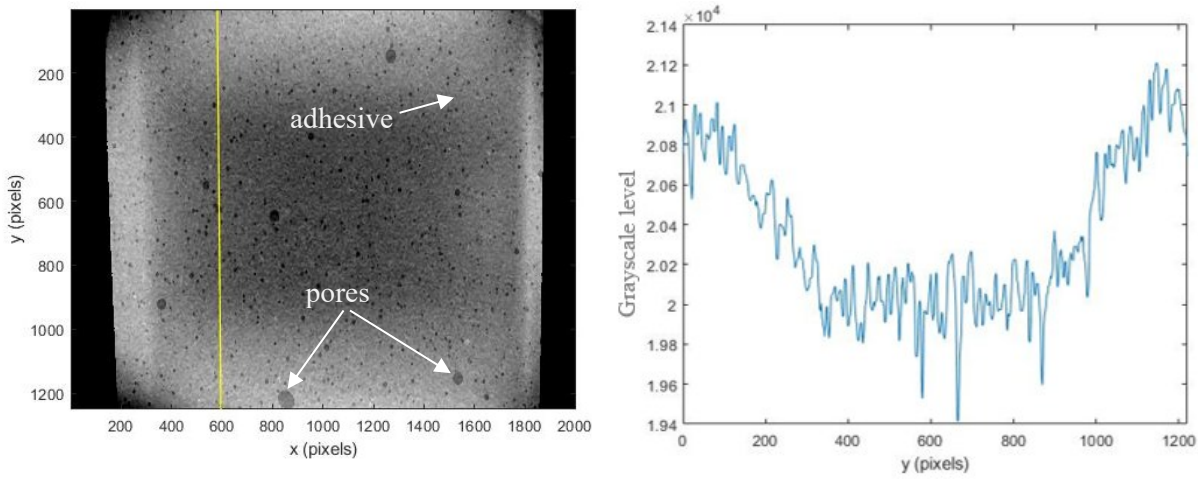

(a) Slice in the middle of the adhesive (b) Grayscale along a path (yellow line on a))

Figure 1. A slice of raw data

Since the raw data obtained from X-ray microthography are encoded in 16 bits and the volumes of the reconstructed samples are quite large, direct analysis of these data is problematic. Thus, the development of the image analysis method and the validation of the architecture of the developed instrument were carried out using the artificial radiographs, generated for a given amount of porosity, porosity ratio, contrast and noise. Therefore, to optimize the analysis time, we created a synthetic volume smaller than the volume of the real sample with similar characteristics. The centroid coordinates and radius of these synthetic porosities are randomly distributed and stored for later comparison.

The generated volume has the following characteristics:

- 300x300x100 voxels^3;
- 300 spherical porosities;

- $\gamma_{porosities} = 30$ (gray level value);
- $b_{Z_j}(x, y)$ - Random noise with a standard deviation value of $\sigma = 9{,}62$ (gray level value);
- The porosity ratio of $9.59\ \%$.

Next, we will represent and explain each step during the generation of the synthetic volume. In the first step we start from a volume of 300x300x100 voxels^3 in which we create 300 spherical porosities. The porosities do not intersect and are uniformly distributed between 1 and 15 voxels and their average radius is 3 pixels. The tool developed should help us find these porosities with the greatest precision.

Figure 2a represents a slice of the raw volume created, consisting of a binomial image in which the adhesive and porosity are correctly determined. Based on equation (2), initially the two phases were created with gray level value 1 ($S_{Z_j}(x, y)$=1) for porosity (white pixels in Figure 2a) and 0 for adhesive (the black pixels in Figure 2a). For the image in Figure 2a thus obtained, in Figure 2b we have represented the gray levels corresponding to the trajectory marked in yellow (x = 150 pixels). From there, the volume will be modeled in such a way that the slices obtained are similar to the raw images obtained from the tomography of the samples taking into account the gray level.

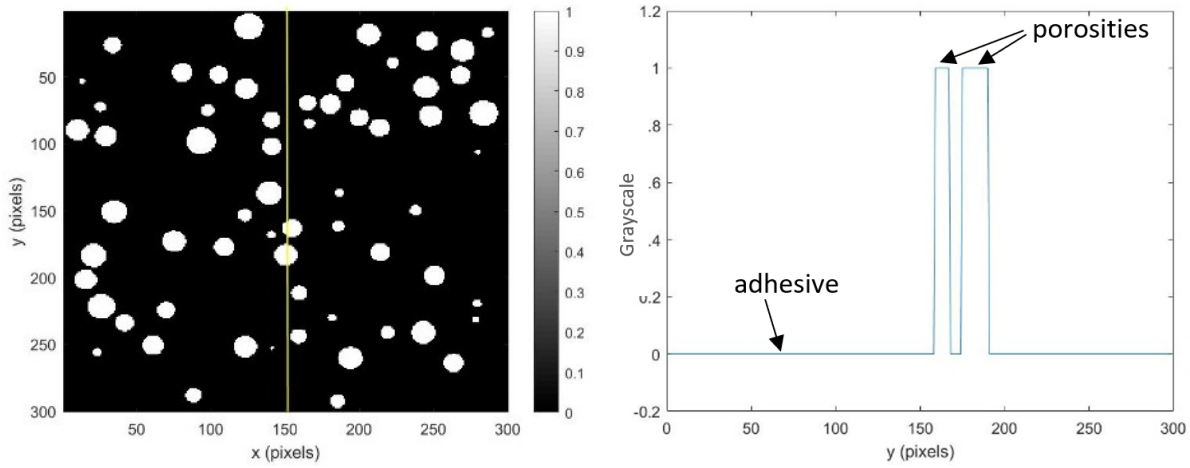

(a) Generated volume slice (b) Grayscale along a path

Figure 2. A slice of generated data (1)

The next step is to assign the actual contrast and gray level intensity values for the two phases of the adhesive. Thus, we assign to the second term of equation (2) ($\gamma_i . p_i(x, y)$) the value 26220 for adhesive and 18560 for porosity. These values were observed from experimental data obtained by X-ray tomography shown as an example in Figure 1b. Figure 3 shows the evolution of the generated image and the signal corresponding to the marked trajectory after the assignment of these values.

The next step in generating our volume is adding random noise. Random noise ($b_{Z_j}(x, y)$) is the third term in our basic equation (2) and influences the generated images and the corresponding gray levels, as shown in Figure 4.

The main interest in our study is the first term of equation (2), the average intensity, $I_{0,Z_j}(x, y)$. The value of this term was determined by an equation of the form:

$$I_{0,Z_j}(x, y) = (ax^5 + bx^4 + cx^3 + dx^2 + ex + f)(gy^2 + hy + i)(jz^2 + kz + l) \quad (3)$$

Where a, b, c, d, e, f, g, h, i, j, k, l are constants and x, y, z represents the coordinates of the points inside the generated volume (300x300x100 voxels^3).

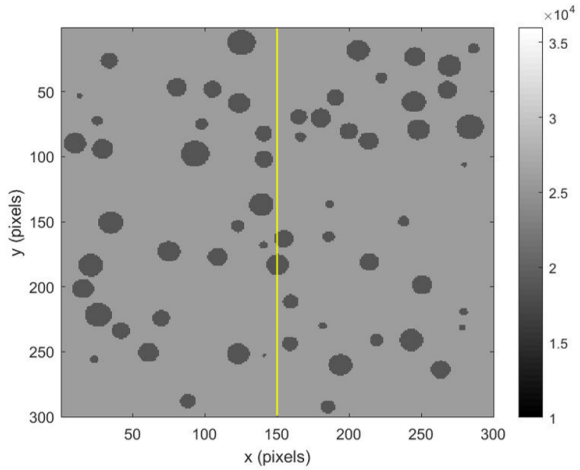

(a) Generated volume slice

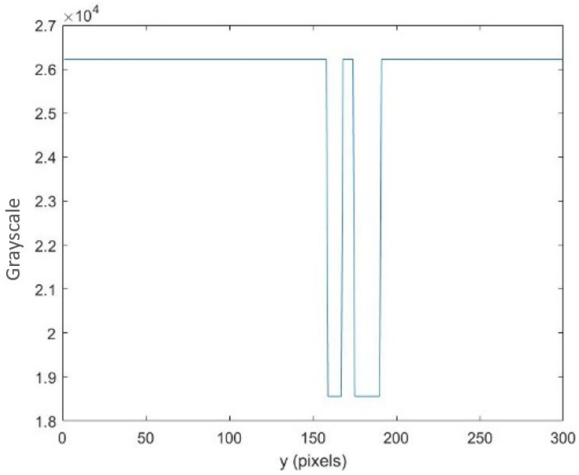

(b) Grayscale along a path

Figure 3. A slice of generated data (2)

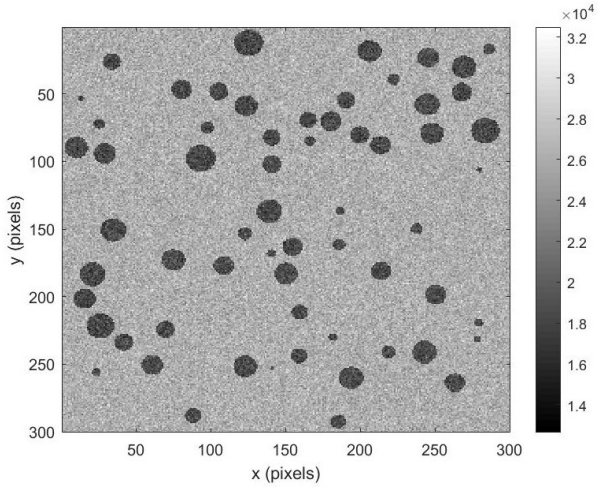

(a) Generated volume slice

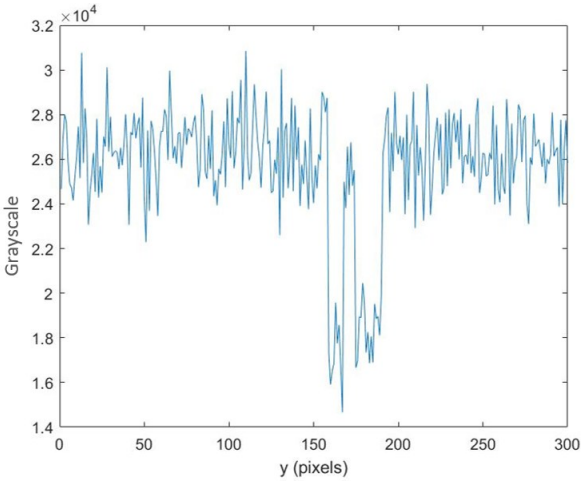

(b) Grayscale along a path

Figure 4. A slice of generated data (3)

Equation (3) of the form describes the surface shown in Figure 5. The average intensity value obtained completes the value of the gray levels established so far in our volume, becoming similar to an actual volume of adhesive. Figure 6 shows the final gray levels obtained for the previously analyzed image after adding I_0.

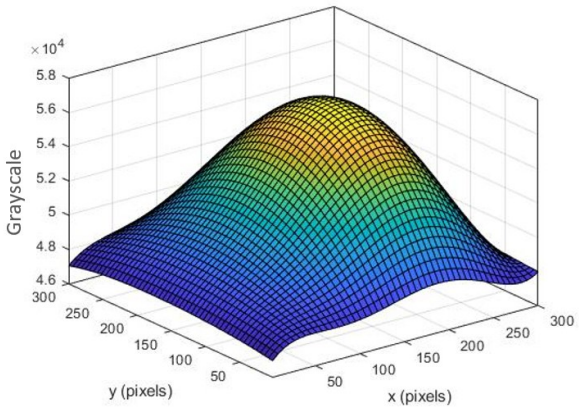

Figure 5. The surface described by the equation of I_0

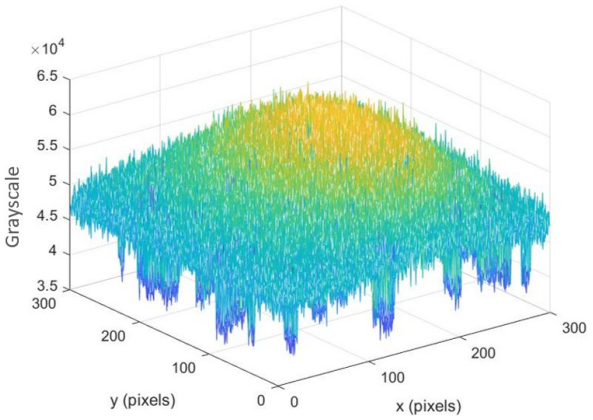

Figure 6. Grayscale for a slice

The final image is shown in Figure 7 which shows the change in path of the signal transmitted by the gray levels. Up to this stage, we can easily separate the two phases present in the adhesive because we can establish a limit between the gray level value corresponding to the adhesive and the gray level value corresponding to the porosities. To choose this limit, Nobuyuk Otsu developed a non-parametric and unsupervised automatic threshold selection method for image segmentation [9]. By this method an optimal threshold is selected by the discriminant criterion in order to maximize the separability of the resulting classes in gray levels. The procedure uses the zero-order and first-order cumulative moments of the gray level histogram (Figure 8).

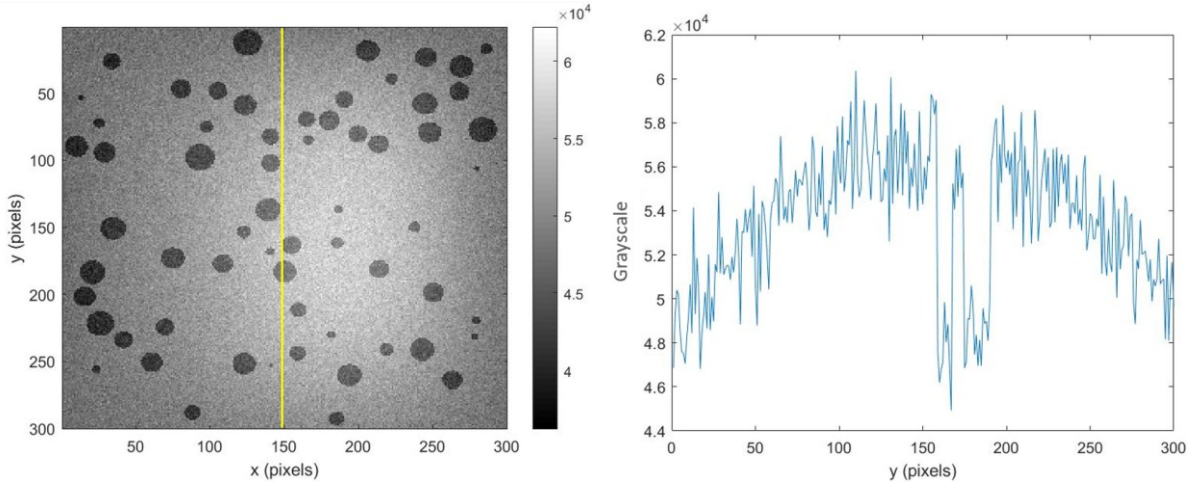

(a) Generated volume slice (b) Grayscale along a path

Figure 7. A slice of generated data (4)

Figure 8a shows the histogram of the generated volume without adding I_0. This is an ideal case where the histogram has a deep, sharp valley between two vertices representing objects and a background, so that the threshold can be chosen at the bottom of this valley. However, for most real images, it is often difficult to accurately detect the valley floor, especially in cases where the valley is flat and wide, soaked in noise, or when the two peaks are extremely unequal in height, they often do not produce a traceable valley. The histogram in Figure 8b represents the case where the average intensity has been added to the gray level. The bottom of the valley is not clear and the gray level boundary between the adhesive and the porosity can no longer be established.

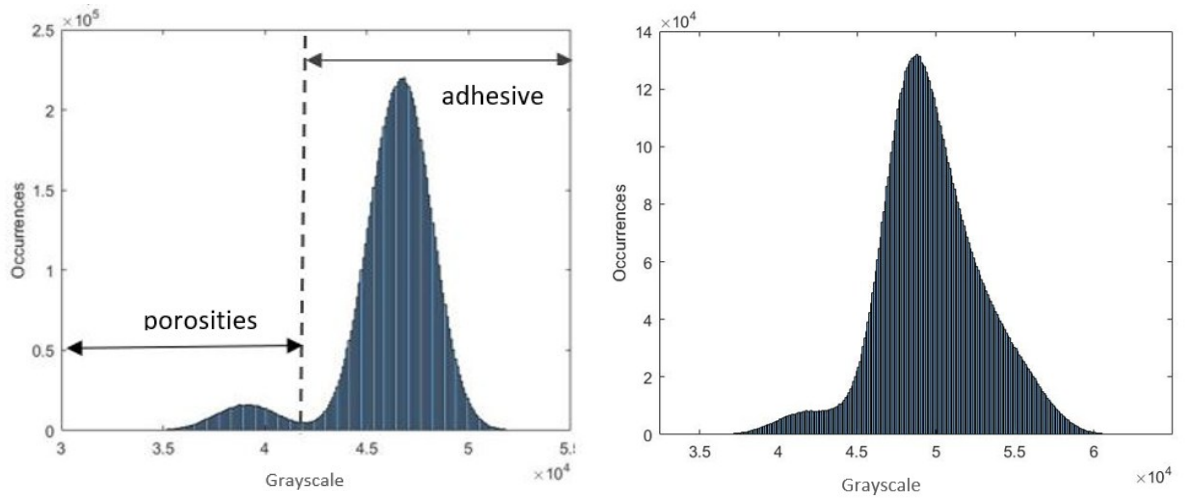

(a) Without I_0 (b) With I_0

Figure 8. Histogram of the generated volume and the threshold calculated using the Otsu method

For a more precise interpretation of the gray level limit between porosity and adhesive, we compared, as an example, two signals of the same trajectory for a slice of the volume without I_0 and respectively with I_0 (Figure 9). In Figure 9a, the red line represents the value found at the bottom of the valley in the histogram of the analyzed volume (gray level = 22 000). The signal represents the gray levels of the slice analyzed at x = 150 pixels and can be interpreted as follows: all points below 22 000 represent the porosities, and all points above this value represent the adhesive. However, the presence of the average intensity in equation (2) almost makes it impossible to separate the two phases. So, we can see in Figure 9b that wherever we place the limit after adding I_0 to the equation, the pores can no longer be separated by the adhesive depending on the gray level value.

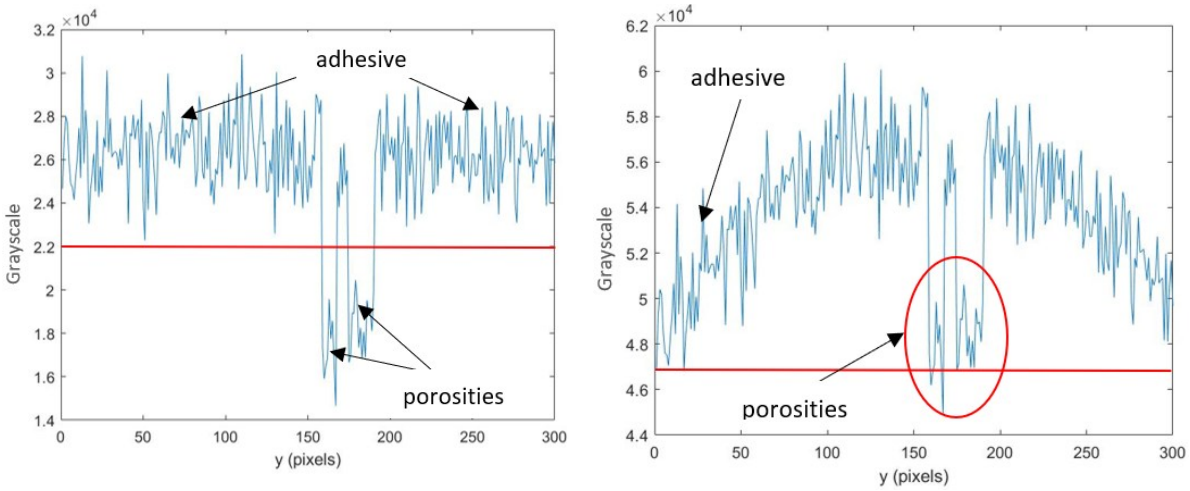

(a) Signal without I_0 (b) Signal with I_0

Figure 9. Grayscale along a path

DEVELOPMENT OF THE TOOL

The main objective of the processing tool is to identify the average intensity I_0 and extract it for each slice of the generated volume. The final images must be clear and we must be able to delineate the pores of the adhesive. By analyzing the synthetic volume of adhesive, we found two methods that allow us to extract I_0. For the sake of clarity, a block diagram representing the development of the proposed analysis tool is shown in Figure 10.

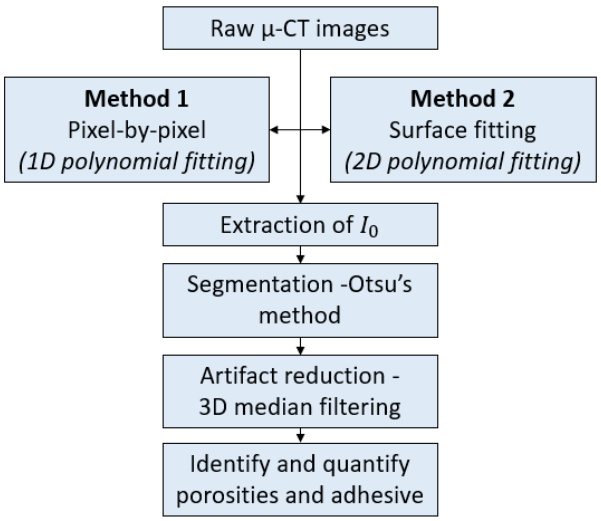

Figure 10. Development of the proposed analysis tool

A first extraction method is the "pixel by pixel" analysis of each slice of the generated volume. This method is based on the search for a polynomial of degree *n* which simulates the trajectory of each gray level signal generated for *x = 1... 300* pixels. For example, Figure 11a shows a slice of the generated volume that we will subsequently analyze to extract the average intensity. We see that the trend of the gray level signal (Figure 11b) for a given trajectory (x = 150) can be described by a polynomial. Extraction I_0 using this method therefore consists of identifying a polynomial of the form:

$$P_{(X)} = a_0 X^n + a_1 X^{n-1} + \cdots + a_{n-1} X + a_n \quad (4)$$

Where: $a_0 \neq 0$; $a_0, a_1, \ldots, a_n$ are the coefficients of the polynomial; X=1…300 is the current pixel index; $P_{(X)}$=$S_{Z_j}(x, y)$ is the corresponding gray level.

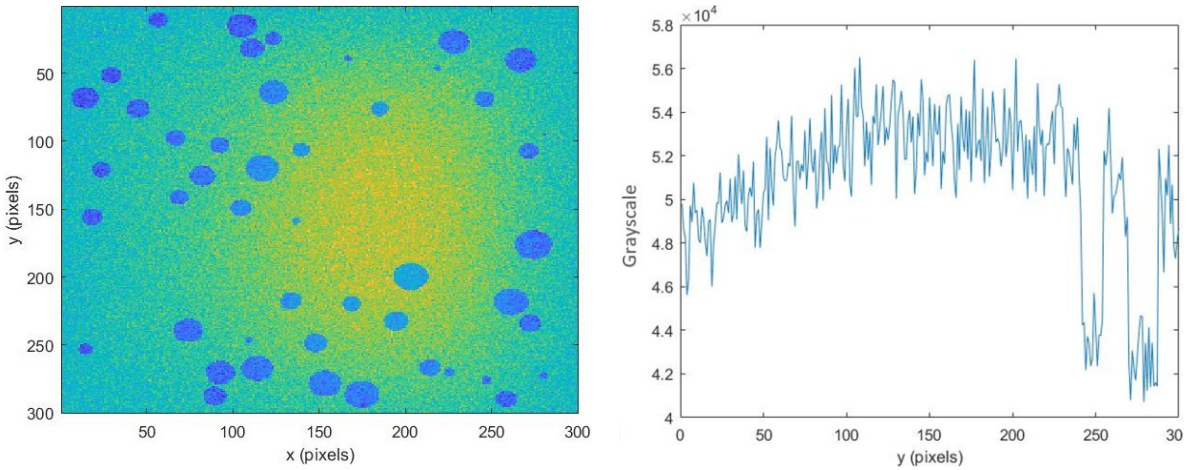

(a) The initial image (b) Grayscale along a path

Figure 11. A slice of generated data (5)

The Matlab software is able to identify this polynomial by calculating the average of all the points representing the gray level value corresponding to a trajectory. The degree of the polynomial represent a parameter to be determined according to the average intensity present in the volume analyzed, according to the calculation method. In this case, for the generated volume, degree 2 of the polynomial was chosen. The polynomial to extract, identified by the software of the analyzed signal, is represented in Figure 12a. The presence of porosity disrupts the trajectory of this polynomial, therefore, in Figure 12b, we can see that the quality of the signal obtained after the extraction of the polynomial is influenced along the zones where the porosities are found.

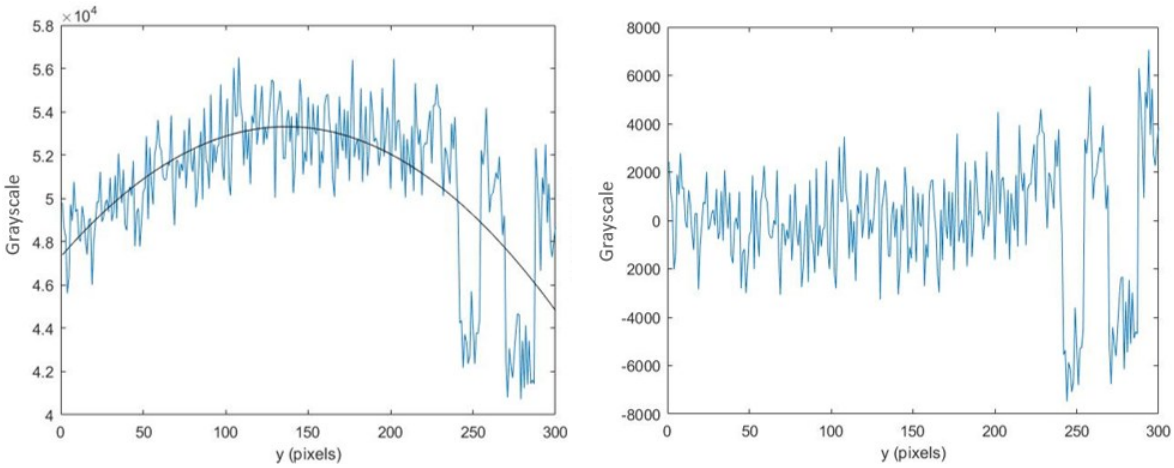

(a) Identification of the first polynomial (b) Signal after extraction of the first polynomial

Figure 12. Extraction of the first polynomial

To correct the signal obtained after the extraction of the 2nd degree polynomial, we apply the same algorithm again, this time changing the approach by choosing the value of the gray levels corresponding to the porosities lower than the value of the corresponding gray levels to the adhesive. From this premise, we will identify a second polynomial based on the average of the upper peaks of the signal highlighted in Figure 13 with red circles. These peaks belong to the adhesive and the trend described by them is not disturbed by the presence of the pores as in the previous step. The 3rd degree of the polynomial was chosen in this case.

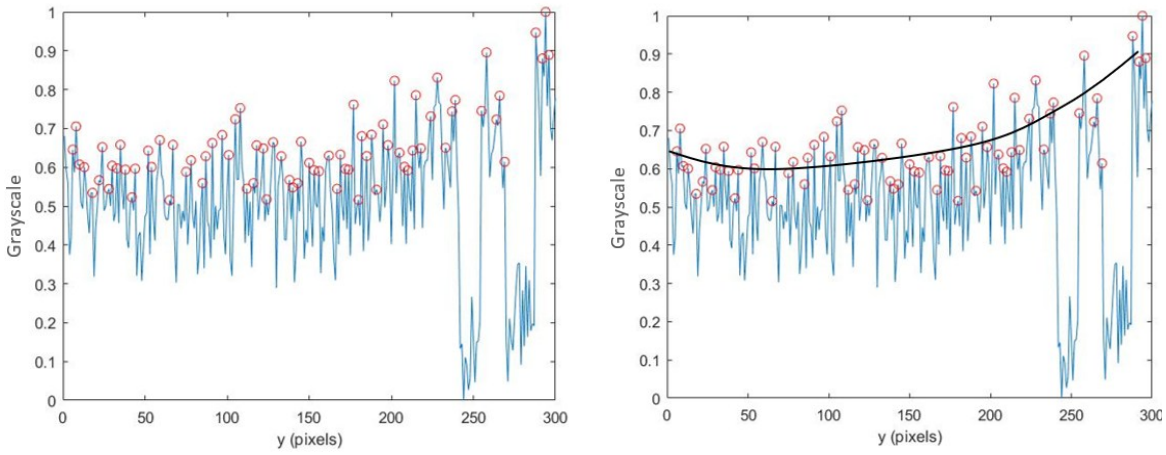

(a) Peak identification (b) Polynomial identification

Figure 13. Identification of the second polynomial

The image we obtain from the extraction of the two polynomials associated with the average intensity is shown in Figure 14a. The quality of the image obtained is visibly improved and we can easily distinguish the pores of the adhesive. Figure 14b shows the gray level signal corresponding to the selected path on the analyzed image. The signal obtained has a linear trend which makes it possible to clearly establish a limit between the values of the gray levels corresponding to the two studied phases.

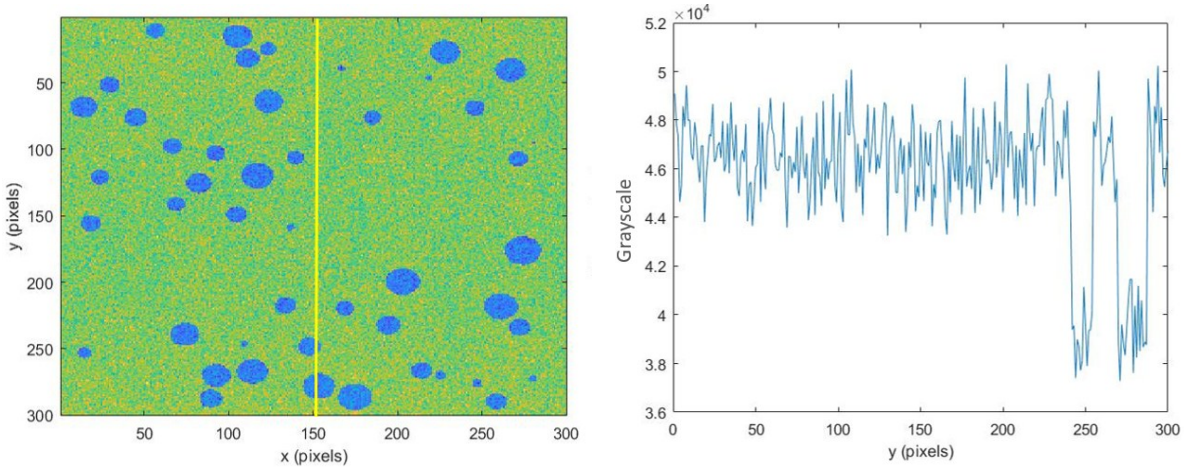

(a) Final image (b) Final signal

Figure 14. A slice of data generated after extraction I_0 by the first method

Since the "pixel by pixel" method of intensity extraction average is satisfactory from the point of view of results obtained, we have developed, in parallel, a second extraction method. This method aims to extract I_0 by optimizing calculation time. Using the first method, each signal of gray level values in an image is analyzed (for $x = 1 \ldots 300$). The second method developed treaty the gray level signals for the whole image. The method is based on identification and extraction of a surface represented by

the average of all points of grayscale values for a slice of the generated volume. The software Matlab can identify this surface as a polynomial shape:

$$S_{(X,Y)} = (a_0X^n + a_1X^{n-1} + \cdots + a_{n-1}X + a_n)(b_0Y^m + b_1Y^{m-1} + \cdots + b_{m-1}Y + b_m) \quad (5)$$

Where: $a_0, b_0 \neq 0$; a_0, a_1,…, a_n, respectively b_0, b_1,…, b_m are the coefficients of the polynomial; *X=1…300, Y=1…300* are the coordinates of the points representing the gray level values for an image; $S_{(X,Y)}$=$S_{Z_j}(x, y)$ is the corresponding gray level.

The degrees of the polynomials which define the surface are the parameters which can be chosen suitably so that the surface found correctly defines the gray levels of the analyzed image. In this case, analyzing the initial image in Figure 11a, given as an example, we can observe in Figure 15 that the surface obtained after choosing degree 5 for the two polynomials perfectly determines the average of the points on the graph.

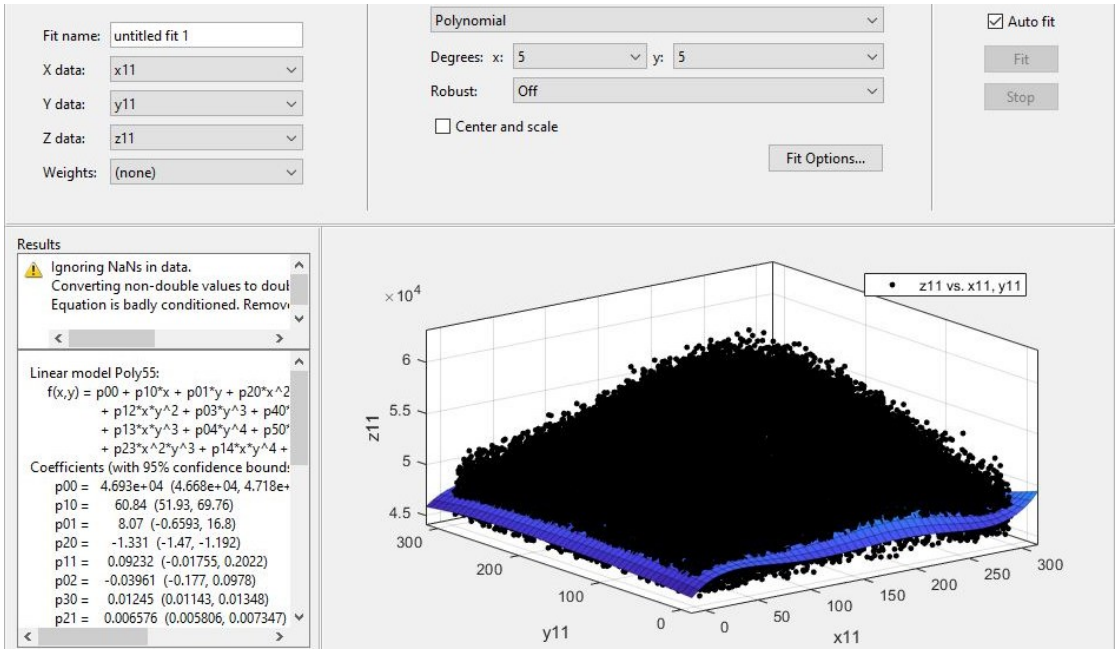

Figure 15. Identification of I_0 by the second method

The effect of extracting I_0 using this method can be seen in Figure 16 where we showed how the raw signal was transformed (Figure 16a) into an uniform signal with a horizontal trend (Figure 16b). The final image shown in Figure 17a is clean and we can easily distinguish the pores of the adhesive.

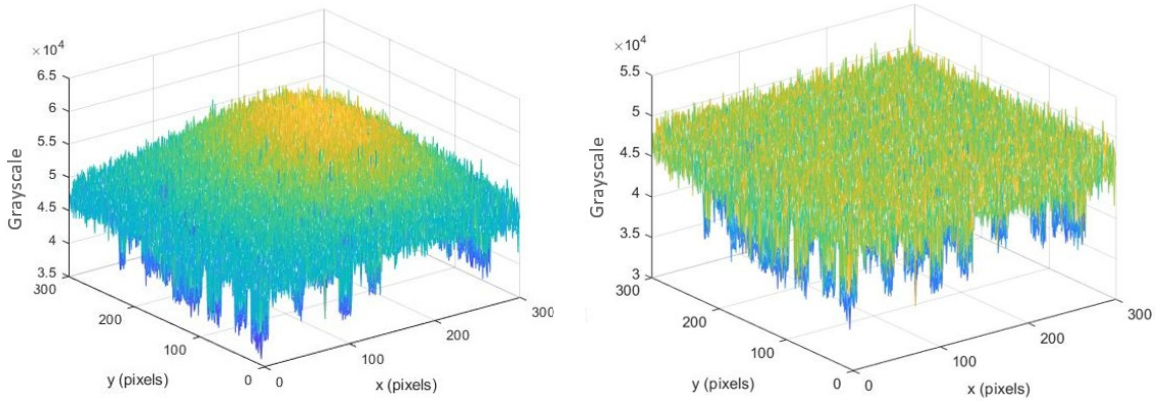

(a) Raw image signal (b) Final image signal

Figure 16. Identification of I_0 by the second method

Comparing the two methods, we observe that the signal along a trajectory obtained with the second method (for x = 150) and shown in Figure 17b is almost identical to the signal obtained with the first method (Figure 14b). Thus, we conclude that both methods gave the desired results, and we can use them in the further analysis of the real data. Given that both methods lead to the same quality of the final image, we will use in the porosity analysis of the volume generated during the second method of extraction of the average intensity for good optimization of calculation times.

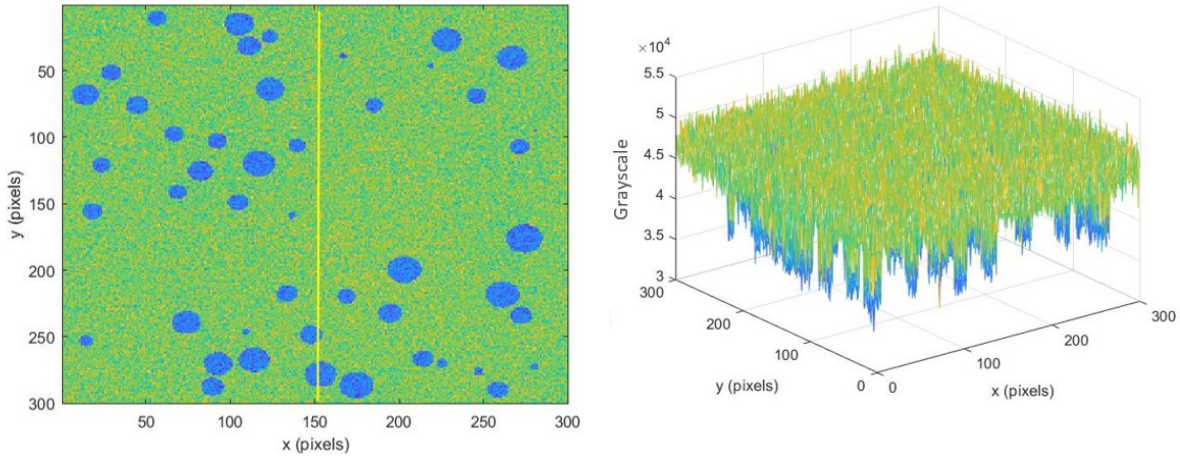

(a) Final image (b) Final signal

Figure 17. A slice of data generated after extraction I_0 by the second method

The final goal of the developed processing tool is to recover the adhesive pores. After extraction I_0, the pores will be recovered by the Otsu method. Also, using the histogram in Figure 18a, we can establish a boundary between adhesive and porosity. Figure 18b shows a binary image in which we find porosities (white pixels) according to the Otsu method. We can see that we find small artifacts that disrupt the quality of the image. These artifacts occur because the valley depicted by the histogram is not perfectly defined. To accentuate this valley and thus recover the porosity without being disturbed by other artifacts, we will apply a 3D median filter using Matlab software [10].

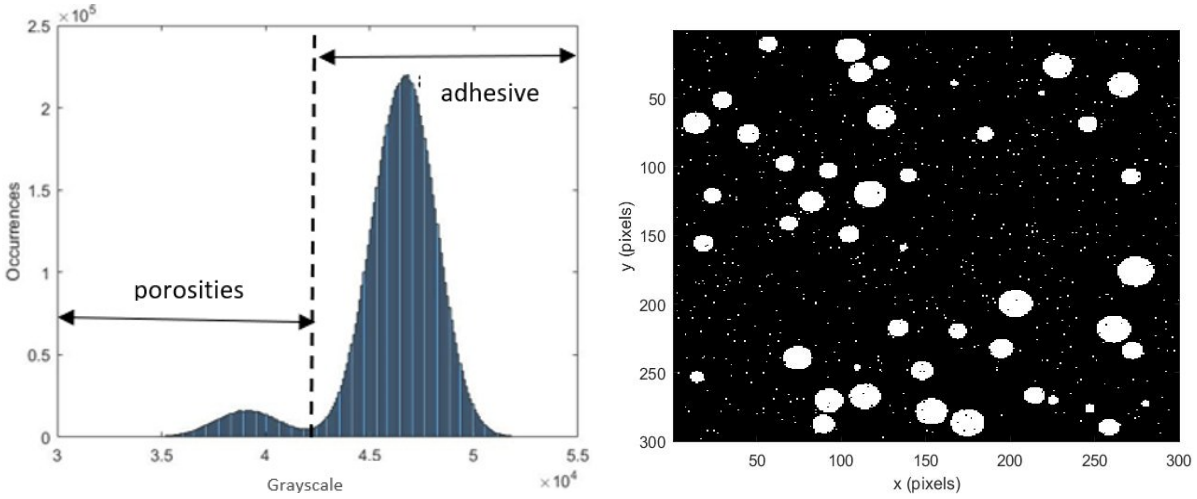

(a) Histogram of the generated volume and the threshold calculated using the Otsu method (b) Porosity found

Figure 18. Porosity analysis (1)

The size of the median filter kernel will determine the minimum size of the segmented features to consider. To remain relatively small compared to the majority of porosities, a kernel size of 7 voxels is chosen. Therefore, all porosity segmented, whose volume is less than 125 voxels^3 (i.e. the volume of

the kernel) will be considered as too uncertain and will therefore be rejected. The chosen filter is three-dimensional to avoid loss of information during filtering.

After 3D filtering of the images, we obtain the histogram shown graphically in Figure 19a where we distinguish a much more pronounced valley than that of the histogram shown previously. Using this histogram, we established a threshold subsequently used in the calculation method for porosity analysis. The porosities finally recovered after the 3D filtering are visible in the image in Figure 19b. The product image is therefore visibly improved because there are no more artifacts, and the pores are well defined.

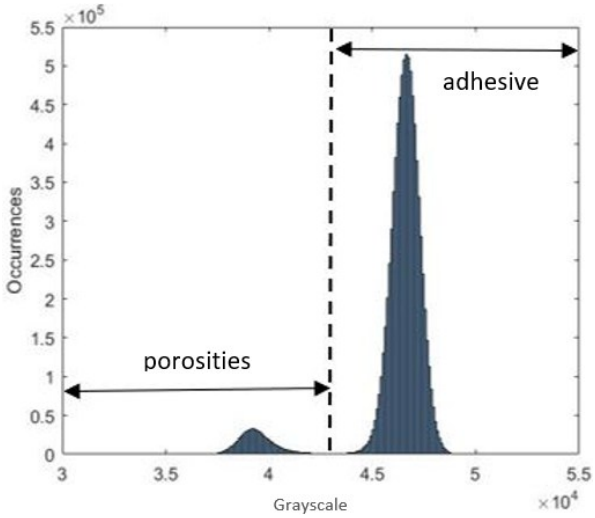

(a) Histogram of the generated volume and the threshold calculated using the Otsu method after filtering

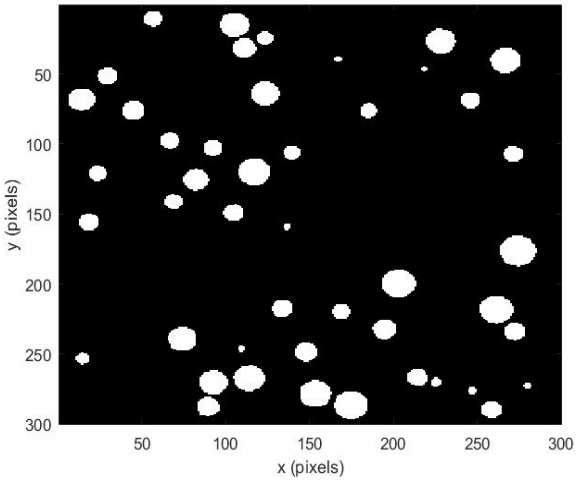

(b) Porosity found after 3D filtering

Figure 19. Porosity analysis (2)

Summarizing and analyzing all the steps of creating the synthetic volume, Figure 20 illustrates the principle of the developed processing tool: starting from a volume in which a certain number of porosities have been generated (Figure 20a), after all its characteristics have been aligned with those of a real adhesive volume (Figure 20b), the average intensity I_0 is extracted (Figure 20c), and finally we find the same porosities as those we generated in the first step (Figure 20d).

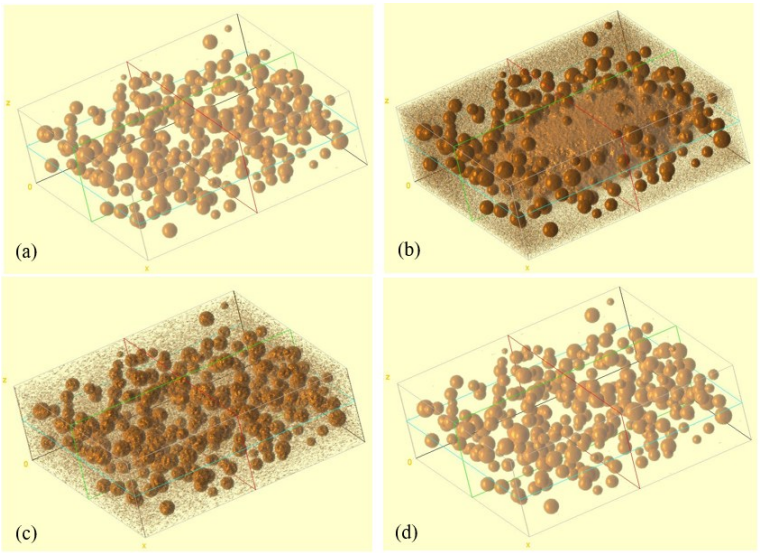

Figure 18. Synthetic volume: (a) Generated porosities; (b) Synthetic volume generated with I_0; (c) Synthetic volume generated after extraction of I_0; (d) Porosities recovered

CONCLUSIONS

The present study addressed a critical issue in the domain of structural adhesive bonding—namely, the presence and influence of porosities within the adhesive layer—by proposing and validating a comprehensive digital processing tool based on X-ray microtomographic data. Given the impact that porosities can have on the initiation and propagation of failure in bonded joints, the ability to visualize and quantitatively assess these defects with high precision is essential for both material characterization and structural integrity evaluation.

To this end, the research introduced a multi-step methodology that begins with the generation of synthetic adhesive volumes. These artificially constructed datasets were designed to simulate real tomographic results while allowing complete control over parameters such as porosity size, localization, intensity contrast and noise. This approach has proven valuable in testing and calibrating image analysis methods before applying it to real data. The cornerstone of the tool's architecture lies in the accurate extraction of average gray level intensity (I_0), which represents a crucial component in differentiating the adhesive phase from porosities. Two extraction methods were explored in depth: (1) a pixel-wise polynomial fitting of intensity variation along defined trajectories, and (2) a global surface-based fitting method using bivariate polynomials to model the full intensity distribution across image slices. Both approaches yielded comparable segmentation accuracy, but the second method demonstrated a clear advantage in terms of computational efficiency, making it the preferred choice for large data sets and real adhesive volumes.

Beyond the intensity correction step, the study implemented Otsu's thresholding method to delineate pore boundaries based on grayscale histogram separation. However, due to real-world signal variability and noise, this step alone was insufficient. To enhance segmentation robustness, a 3D median filter was applied, removing small artifacts and smoothing the volume in a way that preserved relevant porosity features. The post-filtering analysis revealed significant improvement in histogram clarity and pore identification accuracy.

The tool developed through this study enables a complete and semi-automated processing pipeline, including:

- Raw tomographic image import and preprocessing;
- Average intensity extraction and grayscale normalization;
- Noise reduction and artifact suppression;
- Segmentation of porosities with adjustable thresholds;
- Visualization and statistical quantification of pore characteristics (e.g., number, volume, distribution).

Applied to real experimental data, this tool facilitates a more accurate understanding of how manufacturing defects influence adhesive joint behavior. It provides a solid foundation for coupling experimental observations with numerical modeling approaches (such as cohesive zone modeling or finite element simulations), where realistic input data regarding porosity geometry and density are paramount.

From a broader perspective, the results demonstrate that tomographic data, when properly processed, can unlock crucial insights into the integrity of adhesive interfaces. The integration of this tool into experimental workflows can be particularly beneficial in industries such as aerospace, automotive, marine, and energy, where lightweight materials and hybrid assemblies are increasingly employed, and where bonding reliability is paramount.

Looking forward, future developments may focus on:

- Expanding the tool's capabilities for in situ time-lapse tomography to study porosity evolution under mechanical loading;
- Integrating machine learning algorithms to enhance segmentation accuracy and automate threshold selection;
- Applying the methodology to different types of adhesives, joint configurations, and substrates.

In conclusion, the digital tool developed in this work not only provides a robust and efficient framework for porosity analysis in adhesive joints, but also opens the door to more advanced structural diagnostics and material optimization strategies that are essential in high-performance engineering applications.

REFERENCES

[1] Alfonso, L., Badulescu, C., Carrere, N. (2018). Use of the modified Arcan fixture to study the strength of bonded assemblies for automotive applications: effect of different parameters, *In: Journal of Adhesion and Adhesives, Volume 80*, pages 104–114

[2] Dumont, V., Badulescu, C., Adrien, J., Carrere, N., Maire, E. (2019). Experimental Investigation of Porosity in a Bonded Assembly by means of X ray Tomography and Microscopic Observations. *The Journal of Adhesion, Volume 97(6), Issues 1-25*

[3] Tintatu, A., Bidaud, P., Badulescu, C., Le Grognec, P., Adrien, J., Bonnard, G., Maire, E., Bindi, H., Coguenanff, C. (2023). Robust water diffusion modeling in a structural polymer joint based on experimental X-ray tomographic data at the micrometer scale. *Polymer Degradation and Stability, Volume 218, 110594, ISSN 0141-3910*

[4] Tintatu, A., Bidaud, P., Badulescu, C., Le Grognec, P., Adrien, J., Maire, E., Bindi, H., Coguenanff, C. (2023). Understanding of water uptake mechanisms in an epoxy joint characterized by pore-type defects. *The Journal of Adhesion*, *Volume 100(1), Issues 1–33*

[5] Dumont, V. (2020). On the durability of structural adhesive bonds in thermal environments: application to space-oriented optical systems. *PhD thesis*

[6] Dumont, V., Badulescu, C., Stamoulis, G., Adrien, J., Maire, E., Lefèvre, A., Thévenet, D. (2021). On the Effect of the Curing Cycle on the Creation of Pores in Structural Adhesive Joints by Means of X-Ray Microtomography. *The Journal of Adhesion*, *Volume 97(12), 1073–1106*.

[7] Salvo, L., Suéry, M., Marmottant, A., Limodin, N., Bernard D. (2010, November–December*).* 3D imaging in material science: Application of X-ray tomography, *Comptes Rendus Physique, Volume 11, Issues 9–10,* pages 641–649

[8] Tintatu, A., Badulescu, (2024). Analysis of porosity evolution in a bonded assembly under tensile-shear stress by X-ray mictrotomography. *Scientific Bulletin Automotive, Volume 33*

[9] Otsu, N. (1979). A Threshold Selection Method from Gray-Level Histograms. *IEEE Transactions on Systems, Man, and Cybernetics 9.1*, pages 62-66

[10] Gallagher, N. C., Wise, G. L. (1981) A Theoretical Analysis of the Properties of Median Filters. *IEEE Trans. Acoust. Speech Signal Process*., *Volume 29*, *1136–1141*.